ANALYSIS OF THE APPLICATION OF THE NEAR-FAULT GROUND MOTION FUNCTIONS

J. Györgyi
Budapest University of Technology and Economics, H-1521 Budapest, Műegyetem rkp. 3
E-mail of corresponding author: jgyorgyi@enternet.hu

ABSTRACT

Near-fault ground motions are characterised, in case of inter-plate earthquakes, by pulse actions with large periods and velocities, and moderate ones in case of intra-plate earthquakes. Examining the velocity records of many near-fault earthquakes results the ground velocity and pulse period are connected on the base of formula of Krawinkler et al [1] with some corrections for small pulse periods. Using the main characteristics of near-fault ground motions, some research works have proposed simple models of pulse shapes that describe these ground motions. The velocity function was performed by Menun & Fu [2], but calculating the displacement and acceleration functions from it, we find some problem in them. Therefore we suggested the new possibility to modelling the velocity pulses to use algebraically functions [3], which have the same maximum of velocity and the same period then function of Menun & Fu, but the displacement and acceleration functions are compatibility with the velocity function. In this paper we calculated the acceleration functions, using the simulation records of recorded response, which was generated by Fu & Menun [5].

CALCULATING BY MAGNITUDO DEPENDENT VELCITY FUNCTIONS

Examining the velocity records of many near-fault earthquakes results the forward type in Figure 1a, for thrust faults with a main single pulse in the forward direction, forward and back type in Figure 1b, for strike-slip faults in the parallel direction of the rupture and multiple pulses in Fig. 1c for strike-slip fault in the normal direction of the rupture.

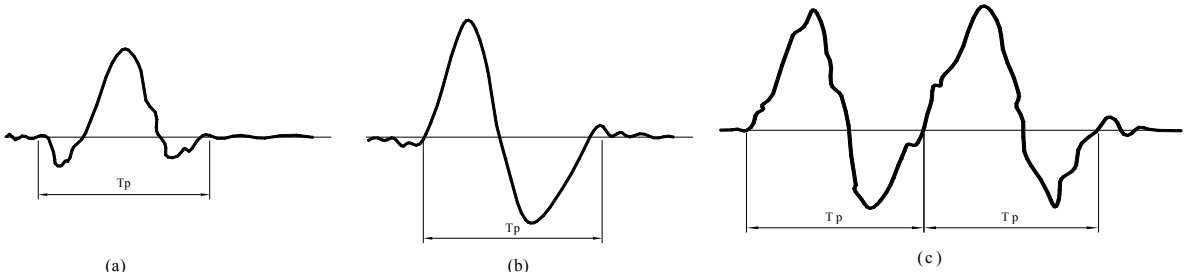

Fig.1: Main types of velocity pulses

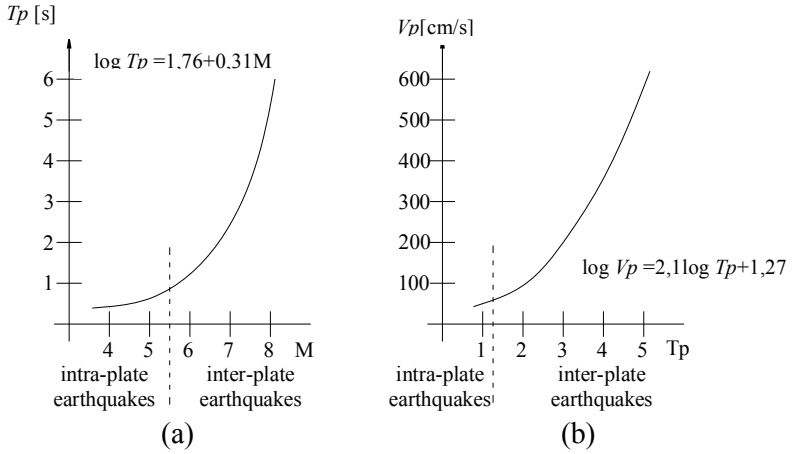

Fig. 2: Ground velocities and pulse periods

Ground velocity and pulse period are connected in Fig. 2, plotted on the base of formula of Krawinkler et al [1]. Firstly the pulse period depends on the magnitude in Fig. 2a. The same relationships exist between ground motion velocities and pulse periods in Fig. 2b. Using the main characteristics of near-fault ground motions, some research works have proposed simple models of pulse shapes that describe these ground motions. Some typical near-fault ground motions are in the Fig. 3.

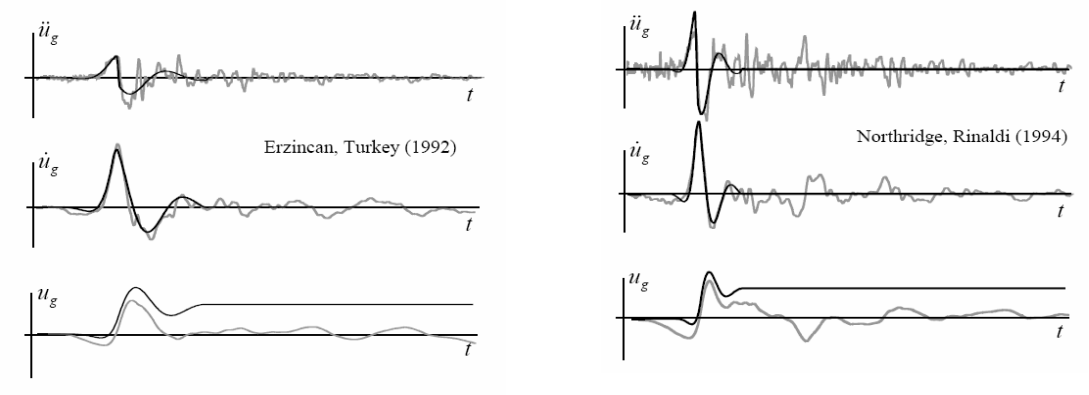

Fig. 3: Typical near-fault ground motions

The main problem of using simplified models for ground motion is if these can substitute, in structural analysis, the recorded ground motions. The results of studies were performed by Menun and Fu [2]. His formula is in (1). Here V_p and T_p characterize the amplitude and period of the velocity pulse, n_1, n_2 are the form parameters, t_0 is the time at which the pulse starts

$$\dot{u}(t) = V_p \exp\left[-n_1\left(\frac{3}{4}T_p - t + t_0\right)\right]\sin\left[\frac{2\pi}{T_p}(t-t_0)\right] \qquad t_0 < t \le t_0 + \frac{3}{4}T_p$$

$$= V_p \exp\left[-n_2\left((t-t_0) - \frac{3}{4}T_p\right)\right]\sin\left[\frac{2\pi}{T_p}(t-t_0)\right] \qquad +\frac{3}{4}T_p < t \le t_0 + 2T_p \qquad (1)$$

$$= 0 \qquad \text{otherwise.}$$

If we use this velocity function there are some problems in the displacement and acceleration functions. There is the jumping in acceleration function and displacement at the end of motion. Therefore we suggested the new possibility to modelling the velocity pulses is to use algebraically functions [3]. In the Figure 4a-c we can see the original and approximate functions.

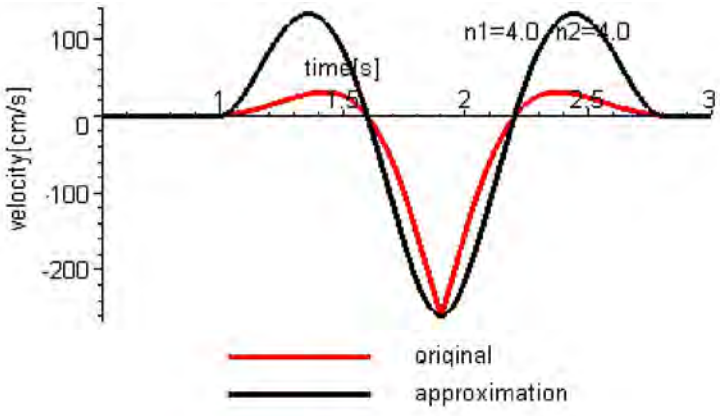

Fig.4a: The velocity functions

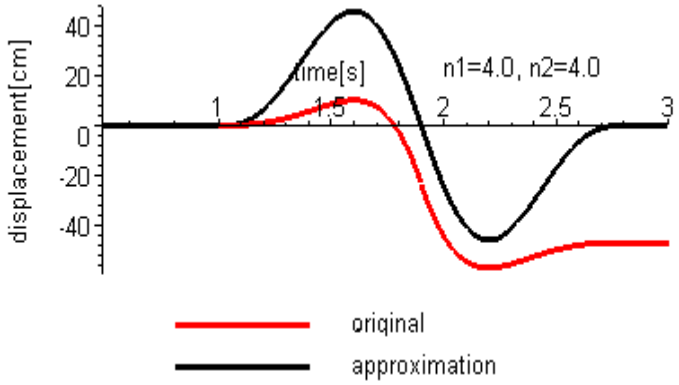

Fig. 4b: The acceleration functions

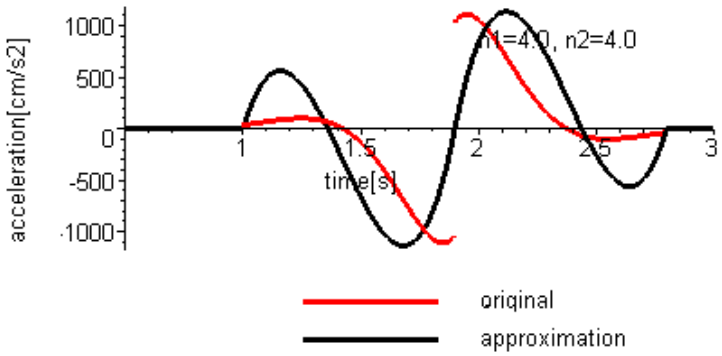

Fig. 4c: The displacement functions

From the displacement and acceleration functions the displacements and internal forces of the structure can be calculated. We calculated a frame structure in [3].

The Fig. 5 and Fig. 6 show the acceleration response spectrums in case of different magnitudes. We can see that the period when is the maximum of the spectrum is different and the ratio of the maximum acceleration and the zero period acceleration is larger than in Eurocode (3.46 > 2.5). It is very interesting that there are periods, where the values of the spectrum at less magnitude are larger than in case of the larger magnitude.

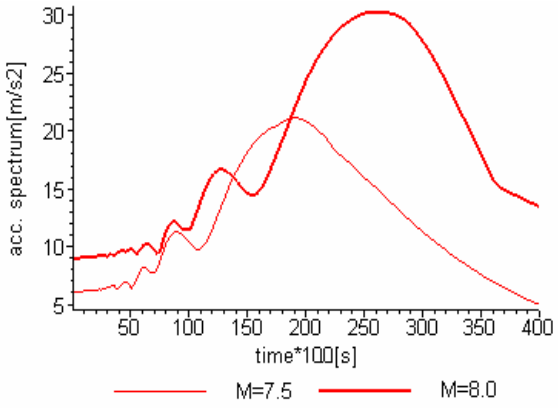

Fig. 5: The acceleration response spectra at M=8.0-7.5

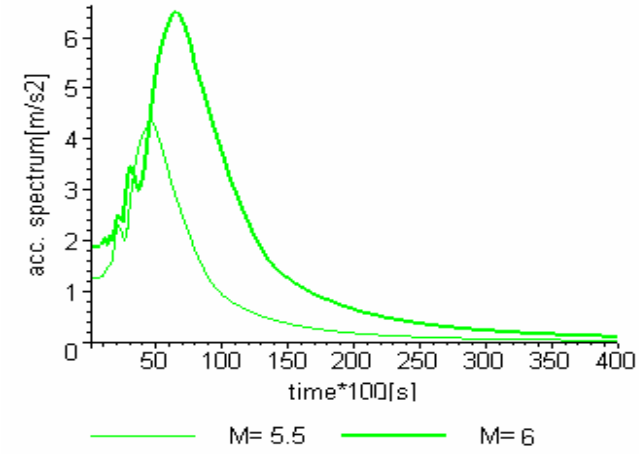

Fig. 6: The acceleration response spectra at M= 6.0-5.5

In the Fig. 7 there are the calculated acceleration response spectra at M=8.0-5.5 and the spectra from the Eurocode 8 in case of M=8.0.

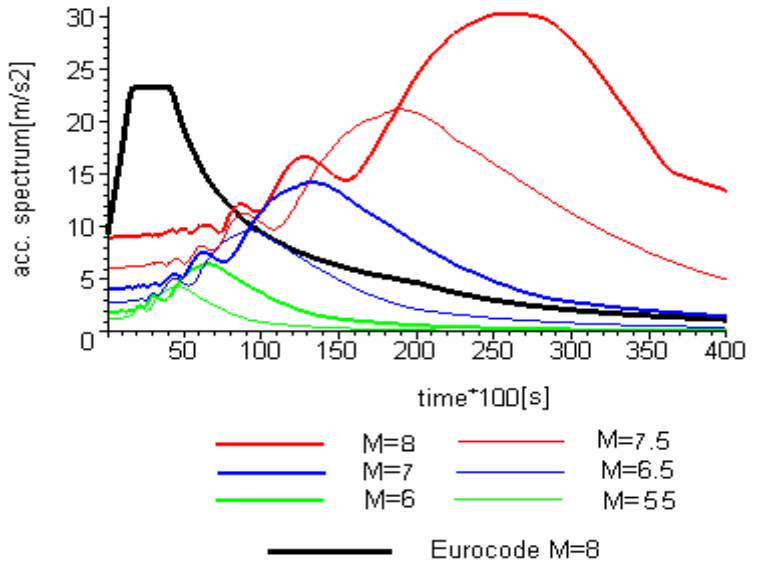

Fig. 7: The acceleration response spectra at M=8.0-5.5 and from Eurocode at M=8.0

We can see that the ground acceleration is same, but very large difference in the time period of maximum value of the Eurocode and calculated spectrum. The peak of the spectrum depends on the magnitude. More results of analysis in [4]

SIMULATION OF NEAR-FAULT GROUND MOTION AT SEIZMIC-ENVIROMENT

In [5] Fu and Menun described a procedure for simulation fault normal near-fault ground motions for the seismic environment (magnitude, distance and faulting mechanism of an earthquake and the soil conditions at the site). The velocity pulse in the synthetic ground motion was idealized in form:

$$v_p(t) = V_p \exp\left[1-\alpha\left(t-t_p\right)-\exp\left(-\alpha\left(t-t_p\right)\right)\right]\sin\left[2\pi\left(t-t_0\right)/T_p\right] \qquad t_0 < t \le t_0 + 2T_p \quad = 0$$

otherwise. (2)

Here V_p and T_p characterize the amplitude and period of the velocity pulse, t_0 is the time at which the pulse starts, α is the shape parameter that defines the growth and decay of the velocity pulse and $t_p = t_0 + 0{,}75T_p$ is the time which the peak velocity occurs. The idealised ground acceleration , which is found by differentiating (2) is:

$$a_p(t) = V_p A_p(t) \cos\left[2\pi(t - t_0)/T_p - \varphi\right] \qquad t_0 < t \le t_0 + 2T_p$$

$$= 0 \qquad \text{otherwise.} \tag{3}$$

where

$$A_p(t) = \exp\left[1 - \alpha(t - t_p) - \exp\left(-\alpha(t - t_p)\right)\right] \sqrt{\left(-\alpha + \alpha \exp\left(-\alpha(t - t_p)\right)\right)^2 + (2\pi / T_p)^2}\ , \tag{4}$$

and $$\varphi = \arctan \frac{-\alpha + \alpha \exp\left(-\alpha(t - t_p)\right)}{2\pi / T_p} \tag{5}$$

Analysis of Kobe earthquake

In Fig. 8 and Fig. 9 show the functions of ground velocity and acceleration in case of earthquake in Kobe (M=6.9) at two different places (R is the distance to the fault rupture).

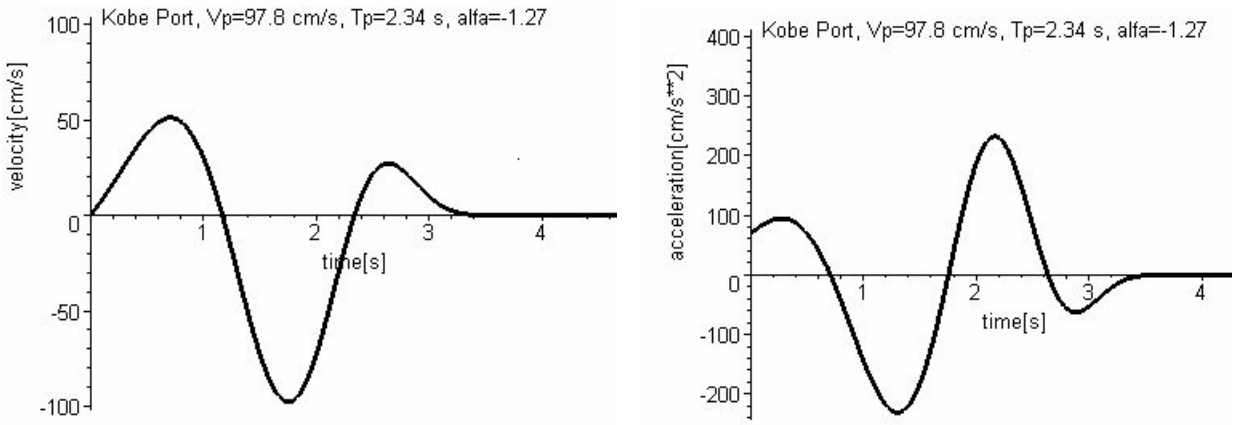

Fig. 8: The velocity and acceleration in Kobe at Port Island (R = 6,6 km)

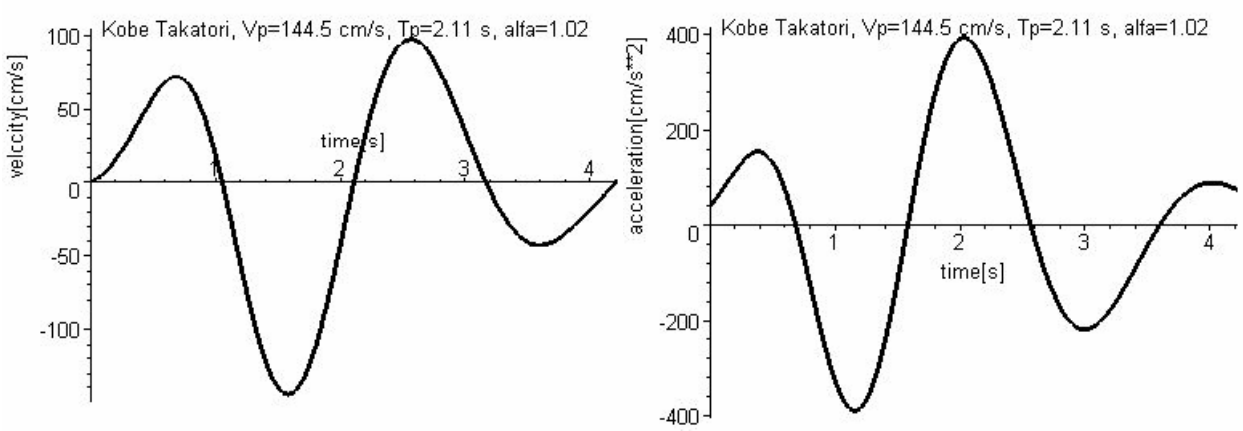

Fig. 9: The velocity and acceleration in Kobe at Takatori Station (R = 4,3 km)

Knowing the acceleration function we can calculate the acceleration response spectrum. In Fig, 10 we can see large difference between the two spectrum. The peak the spectrum of Takatori Station was two times more than other case. (At Fig. 9 the amplitude of velocity was larger by 50% then in Fig, 8.) We have seen the form of the spectrums in Fig. 11. The ratio of the maximum acceleration and the zero period acceleration is 3,3 and 3,66. They are more than in Eurocode, where it was 2,5 in case of horizontal motion and 3.0 at vertical motion.

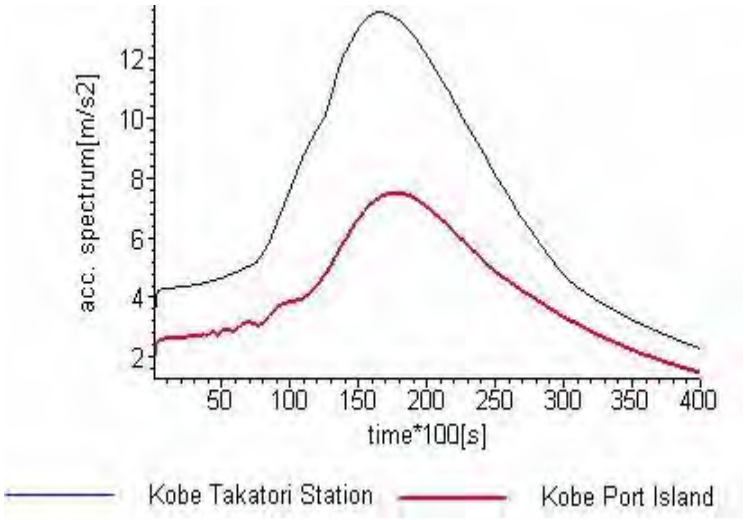

Fig. 10: The acceleration response spectrums in Kobe at two different places

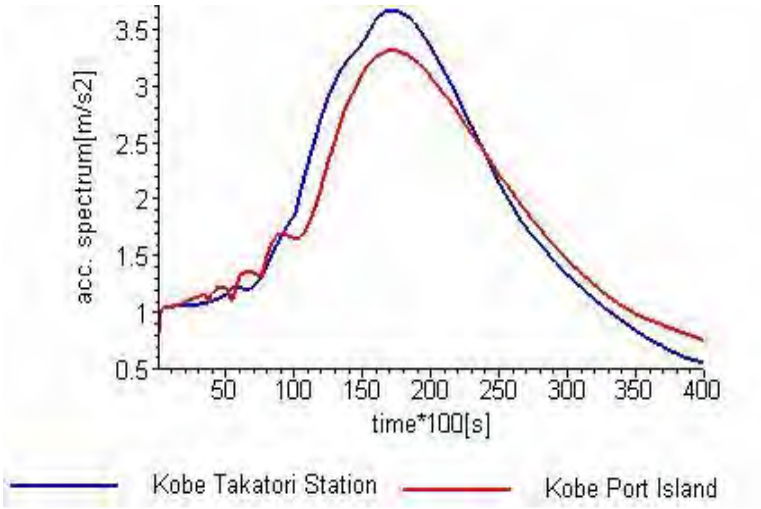

Fig. 11: The form of acceleration response spectrums in Kobe at two different places

Analysis of Northbridge earthquake

In [5] we can see some parameters of Northbridge earthquake - where the magnitude was 6.7 - at eight difference places. From these we analyse five cases.. The parameters are in the Table 1. The acceleration depends form the $|V_p / T_p|$ parameter.

Table 1: Dates of the Northbridge earthquake

The place of measuring	R [km]	V_p [cm/s]	T_p [s]	α	$\lvert V_p / T_p \rvert$
Canoga park	1.75	-40,3	2,02	-1,12	19,9
Canyon City	4.71	27,2	1,89	0,89	14,4
Sylmar Converter East	5.89	-60,6	3,05	0,67	19,9
Jensen Filter Plant	7.77	69,8	2,83	-0,40	24,7
Newhall - Fire station	8.68	-106,8	0,93	3,54	114,8

In Fig. 12 and Fig. 13 show the functions of ground velocity and acceleration functions in case of Canyon City and Newhall. We can see that the acceleration in Newhall was six times more than in Canyon City.

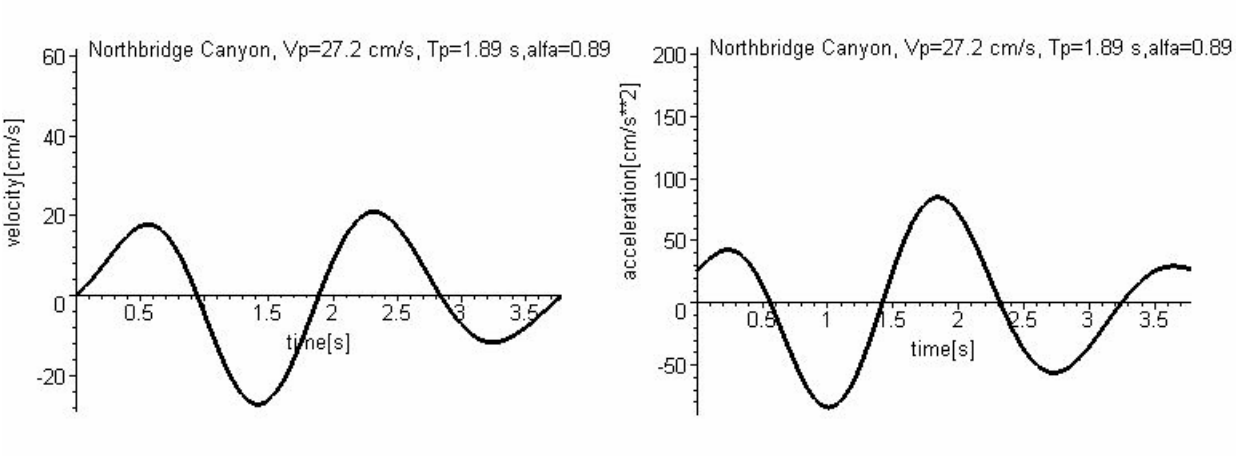

Fig. 12: The velocity and acceleration in Canyon City

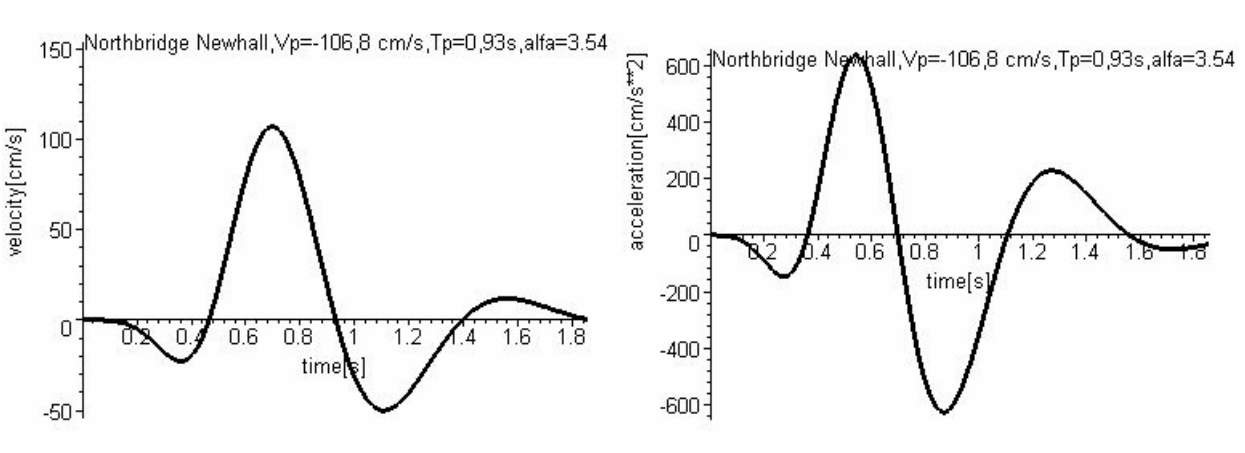

Fig. 13: The velocity and acceleration in Newhall

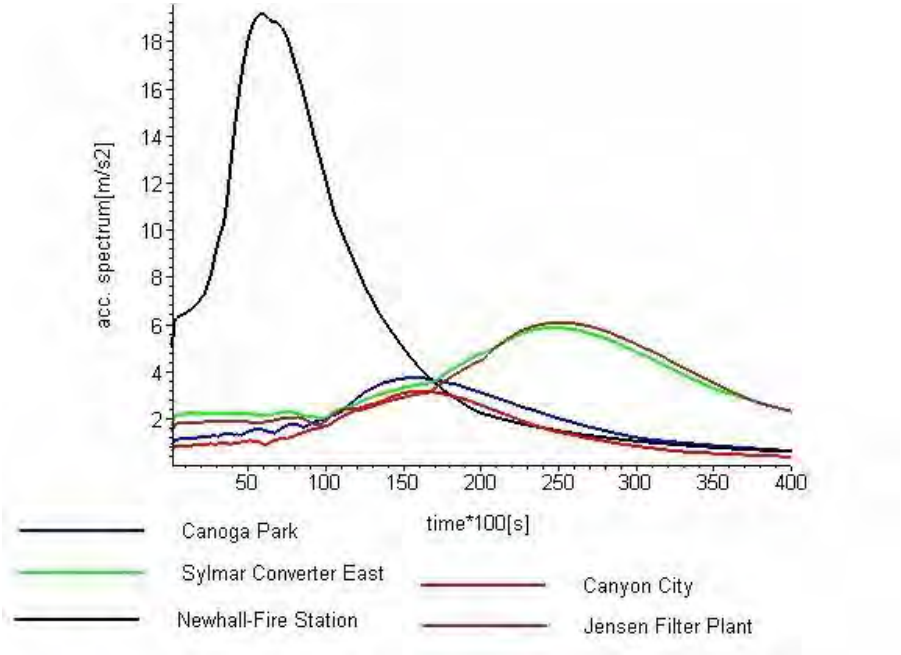

Fig. 14: The acceleration response spectrums in Northbridge at five different places

The Fig. 14 shows the acceleration response spectrums. We can see, that the spectrum at Newhall has large values. In the Fig.15 are the forms of spectrum. The ratio of the maximum acceleration and the zero period acceleration is between the 2,82 and 3,93. They are more than in Eurocode in this case too. The periods, where the values of the spectrum are maximum are between 0,58 and 2,46 s. (In Eurocode they are between 0,15 and 0,80).

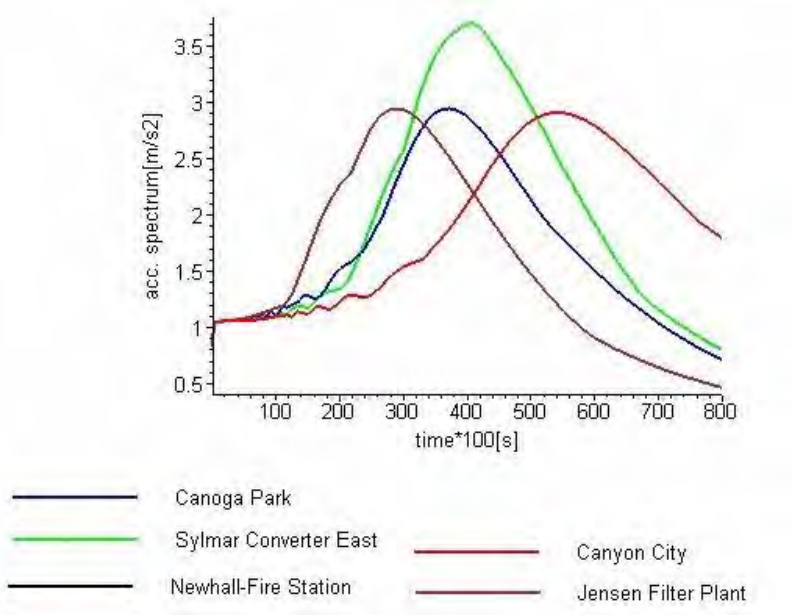

Fig. 15: The forms of acceleration response spectrums in Northbridge at five different places

CONCLUSION

The first part we calculated the acceleration response spectra in case of different magnitude using the [1] and [3]. The magnitudes were changing between 5.5 M and 8.0 M. We found that the period when is the maximum of the spectrum is larger than in the Eurocode and depends from the magnitude. The ratio of the maximum acceleration and the zero period acceleration is larger than in Eurocode (3.46 > 2.5) too, but that is independent from magnitude. In the second part we calculated the near-fault ground motions in case of same magnitude but at different seismic environment (distance of the fault and the soil conditions at the site). The ratio of the maximum acceleration and the zero period acceleration was changing between the 2,82 and 3,93.

REFERENCES

[1] Medina, R., Krawinkler, H., Alavi, B.: "Seismicity drift and ductility demands and their dependence on ground motion". *US –Japan Seminar on Advance Stability and Seismicity Concepts for Performance-Based Design of Steel and Composite Structures*, Kyoto, Japan, 2001.

[2] C. Menun, Q. Fu, "An analytical model for near/fault ground motions and the response of SDOF system". *13th U.S. National Conferences on Earthquake Engineering*. Boston, USA, 2002.

[3] J. Györgyi, V. Gioncu, M. Mosoarca, "Behaviour of steel MRFs subjected to near-fault ground motions". In F. M. Mazzolani & A. Wada, editors, STESSA 2006*, Behaviour of Steel Structures in Seismic Areas*, 129-136. Yokohama, Japan, 2006.

[4] J. Györgyi, "Corrected Ground Motion Functions in the Case of a Near-Fault Earthquake", *The Tenth Int. Conf. on Computational Structures Technology*, #paper 326, pp.1-10, Valencia, Spain, 2010

[5] Q. Fu, C. Menun, "Seismic environment-based simulation of near-fault ground motions". *13th Word Conferences on Earthquake Engineering*. Paper No. 322, Vancouver, B. C., Canada, 2004.